

Supporting Information

Fluorescence Activation Imaging of Cytochrome c Released from Mitochondria Using Aptameric Nanosensor

Ting-Ting Chen,^a Xue Tian,^a Chen-Liwei Liu,^a Jia Ge,^a Xia Chu,^{a,*} Yingfu Li^b

^a State Key Laboratory of Chemo/Bio-Sensing and Chemometrics, College of Chemistry and Chemical Engineering, Hunan University, Changsha, 410082, P. R. China

^b Department of Biochemistry and Biomedical Sciences, McMaster University, Hamilton, L8S 4K1, Canada

Email: xiachu@hnu.edu.cn

ADDITIONAL EXPERIMENTAL DETAILS

Instruments and Characterization. Fluorescence spectra and fluorescence anisotropy spectra were recorded at room temperature in a 100 μ L quartz cuvette on Fluoromax-4 spectrofluorometer (Jobin Yvon, USA) with excitation at 664 nm. The slit was set to be 5 nm for both the excitation and the emission. The UV-visible (UV-vis) absorption spectra were measured in a quartz cell with an optical length of 1 cm using a UV-2550 spectrometer (Shimadzu, Japan) with a wavelength interval of 2 nm. Fourier transform infrared (FT-IR) spectra were collected on a Nicolet Nexus 670 FTIR spectrometer (Nicolet, USA). The topological morphologies of GO were obtained using an atomic force microscopy (Bruker, Germany). All fluorescence images were acquired using an oil dipping objective (100 \times) on a confocal laser scanning fluorescence microscope setup consisting of an Olympus IX81 inverted microscope with an Olympus FV1000 confocal scanning system.

Synthesis of Folate-NHS. Folate-NHS was synthesized according to a procedure reported previously.¹ Briefly, folate (0.5 g) was dissolved in a mixture of 9.75 mL DMSO and 0.25 mL triethylamine. After NHS (0.26 g) and EDC (0.47 g) added successively, the reaction mixture was stirred overnight at room temperature. The byproduct, dicyclohexylurea, was removed by filtration. The solution was concentrated by evaporation under reduced pressure, followed by addition of ethyl ether (20 mL). The resulting yellow precipitate, Folate-NHS, was washed three times with ethyl ether, dried under vacuum, and stored at -20 $^{\circ}$ C for future use.

Preparation of PEGylated GO. GO nanosheets were firstly carboxylated following a procedure we reported previously.² The resulting carboxylated GO nanosheet (~ 2 mg mL⁻¹) was dispersed in water and sufficiently sonicated for 1 h in an ice bath followed by the reaction with 2.2 mM EDC and 1.5 mM Sulfo-NHS for 2 h in 0.1 M phosphate buffer (PB, pH 7.4) to activate the carboxyl groups. The reaction mixture was incubated with NH₂-PEG-NH₂ (2 mg mL⁻¹) for 2 h at room temperature followed by standing overnight at 4 $^{\circ}$ C. Excess NH₂-PEG-NH₂ was removed by dialyzing for 48 h. The resulting PEGylated GO (~ 2 mg mL⁻¹) was dispersed in 0.1 M PB (pH 7.4). The PEGylated GO was added with folate-NHS (2 mg) and allowed the reaction for 2 h under sonication, followed by dialysis against ultrapure water for 48 h to remove excess folate-NHS. The obtained PEGylated GO nanosheets with folate modifiers were diluted to a concentration of ~ 1 mg mL⁻¹ with ultrapure water and stored at 4 $^{\circ}$ C for future use.

The PEGylated GO with FAM and folate modifiers were synthesized by mixing PEGylated GO (~ 2 mg mL⁻¹) in 0.1 M PB (pH 7.4) with FAM-NHS (1.15 mg) and folate-NHS (1 mg) followed by

incubation in an ice bath for 2 h under sonication. Then, the mixture was allowed to react under stirring overnight at room temperature, followed by dialysis against ultrapure water for 48 h to remove excess folate-NHS and FAM-NHS. The purified product, PEGylated GO with FAM and folate modifiers, was diluted to a concentration of $\sim 1 \text{ mg mL}^{-1}$ with ultrapure water and stored at 4°C for future use.

The PEGylated GO with FAM modifiers were synthesized by mixing PEGylated GO ($\sim 2 \text{ mg mL}^{-1}$) in 0.1 M PB (pH 7.4) with FAM-NHS (2 mg) followed by incubation in an ice bath for 2 h under sonication. Then, the mixture was allowed to react under stirring overnight at room temperature, followed by dialysis against ultrapure water for 48 h to remove excess FAM. The purified product, PEGylated GO with FAM modifiers, was diluted to a concentration of $\sim 1 \text{ mg mL}^{-1}$ with ultrapure water and stored at 4°C for future use.

The coverage of PEG on GO nanosheets was determined using the PEGylated GO with FAM modifiers based on the absorption peak of FAM at 494 nm with reference to a standard FAM solution in ultrapure water, assuming that the PEGs were completely conjugated with FAM. The absorbance at 494 nm was 0.3517 for $\sim 1 \text{ mg mL}^{-1}$ PEGylated GO. According to the specific surface area $\sim 705 \text{ m}^2 \text{ g}^{-1}$ for GO,³ the coverage of PEG on GO surface was estimated to be $\sim 8.4 \times 10^{11}/\text{cm}^2$. Based on the average area of a single GO nanosheet (assuming an average nanosheet diameter of $\sim 75 \text{ nm}$), the number of PEG molecules on a single GO nanosheet was estimated to be ~ 47 . Likewise, the number of aptamer molecules on a single GO nanosheet was estimated to be ~ 14 according to its coverage of $\sim 3.1 \times 10^{11}/\text{cm}^2$.

Cytoplasmic protein extraction. Cytoplasmic protein extraction from Hela cells was performed directly according to the protocol indicated in the Cytoplasmic and Mitochondrial Protein Extraction Kit. Briefly, cells ($\sim 6.5 \times 10^6$) were suspended with 0.5 mL of $1\times$ Cytosol Extraction Buffer Mix containing DTT and Protease Inhibitors. After incubated on ice for 10 min, the cells were homogenized adequately to obtain a disruption rate $>90\%$ while not to damage the mitochondrial membrane. The homogenate was centrifuged at 12000 rpm to precipitate the mitochondrial, and the supernatant was collected as cytosolic fraction. The cytosolic fraction was retained frozen at -80°C before used.

Because DNA aptamer assembled on PEGylated GO surface could be completely displaced and dissociated from the surface in the cytoplasmic extract buffer, the cytosolic fraction was needed to remove the surfactants or other chemical compound from cytoplasmic extract buffer through ultra-filtration (MW 10000) at 4°C for 10 times using $1\times$ PBS before the next experiment.

Estimation of intracellular concentration of nanoassembly. The determination of intracellular concentration of the nanoassembly was based on our observation that DNA aptamer assembled on

PEGylated GO surface could be completely displaced and dissociated from the surface using the cytoplasmic extract buffer (two ionic detergents and one nonionic detergent in Tris buffer: 25 mM Tris•HCl, pH 7.6, 150 mM NaCl, 1% NP-40, 1% sodium deoxycholate and 0.1% sodium dodecyl sulfate), as shown in Figure S19. The dissociated aptamer exhibited an activated fluorescence signal, which enabled us to determine the concentration of the nanoassembly.

In this assay, Hela cells (FR+, $\sim 3.56 \times 10^5$) were plated on a 35-mm Petri dish with 10-mm bottom well in the folate-free RPMI 1640 medium for 24 h, then incubated with the nanoassembly solution containing 50 nM aptamer and $15 \mu\text{g mL}^{-1}$ PEGylated GO in the folate-free RPMI 1640 medium at 37 °C for 1 h. The incubation solution was collected and concentrated by 10-fold through ultra-filtration (MW 10000). Then, a 10 μL aliquot of the concentrated incubation solution was mixed with 90 μL cytoplasmic extract buffer for 10 min. The fluorescence of the dissociated cy5-tagged aptamer was measured and the concentration of the aptamer was determined using a set of standard solutions of the nanoassembly. The amount of the nanoassembly was estimated based on the difference of the total concentration and the previously determined value. According to the volume of a single Hela cell,⁴ the concentration of nanoassembly uptaken in Hela cells was estimated to be $\sim 148.8 \mu\text{g mL}^{-1}$, which was ~ 10 -fold concentrated in the cells due to the efficient uptake of the nanoassembly in the cells.

References:

1. D. Feng, Y. Song, W. Shi, X. Li, H. Ma, *Anal. Chem.* **2013**, 85, 6530-6535.
2. H. Wang, Q. Zhang, X. Chu, T. Chen, J. Ge, R. Yu, *Angew. Chem. Int. Ed.* **2011**, 50, 7065-7069.
3. Y. Zhu, S. Murali, W. Cai, X. Li, J. W. Suk, J. R. Potts, R. S. Ruoff, *Adv. Mater.* **2010**, 22, 3906-3924.
4. L. Zhao, C. D. Kroenke, J. Song, D. P. Worms, J. J. H. Ackerman, J. J. Neil, *NMR Biomed.* **2008**, 21, 159-164.

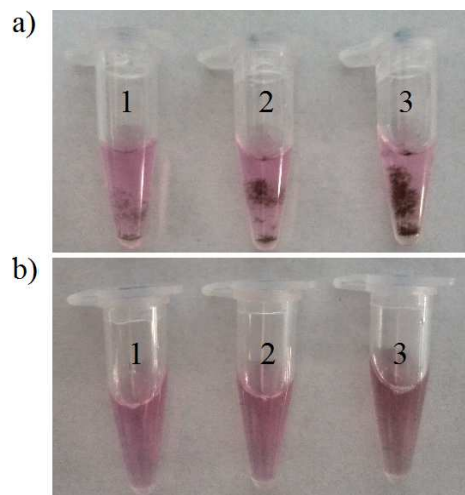


Figure S1. Photographs of the nanoassembly prepared with aptamer-GO nanoassembly (a) and aptamer-PEGylated GO nanoassembly (b) incubated in serum-free RPMI-1640 medium overnight at 4 °C. 1) $10 \mu\text{g mL}^{-1}$ GO concentration, 2) $20 \mu\text{g mL}^{-1}$ GO concentration, 3) $50 \mu\text{g mL}^{-1}$ GO concentration.

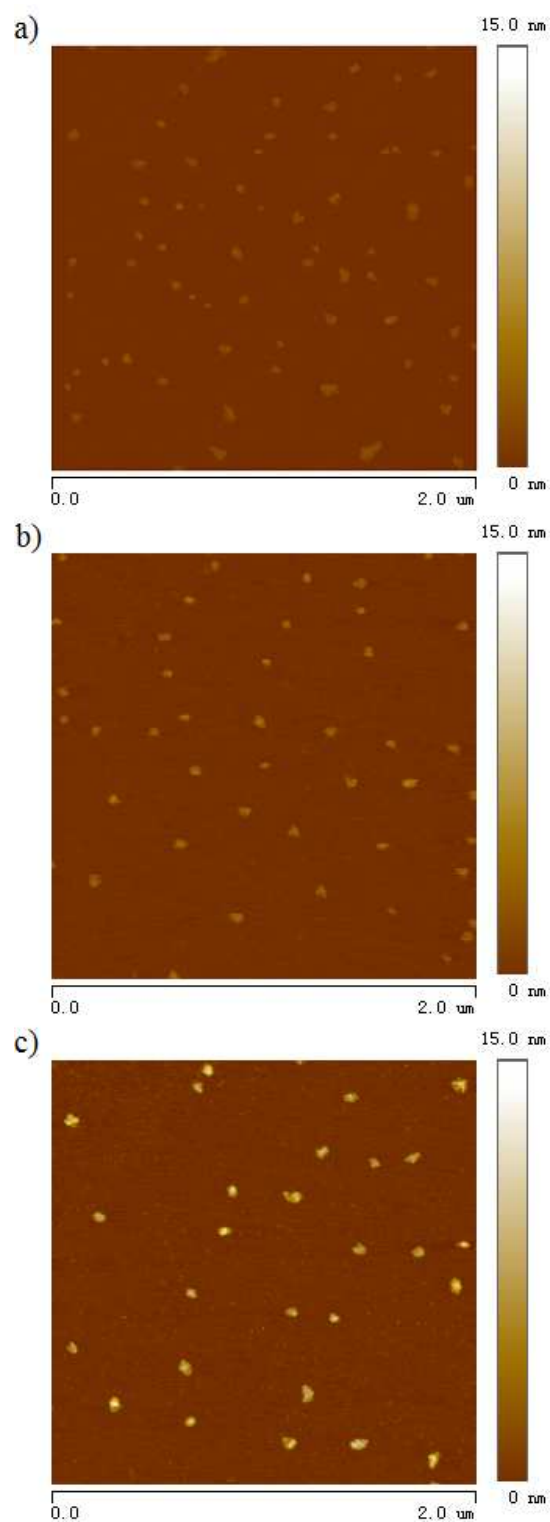


Figure S2. AFM image of GO (a), PEGylated GO (b) and aptamer-PEGylated GO nanoassembly (c). The nanosheets are well mono-dispersed, and typical lateral dimension of the as-prepared GO or its nanoassembly ranged from 50 to 100 nm.

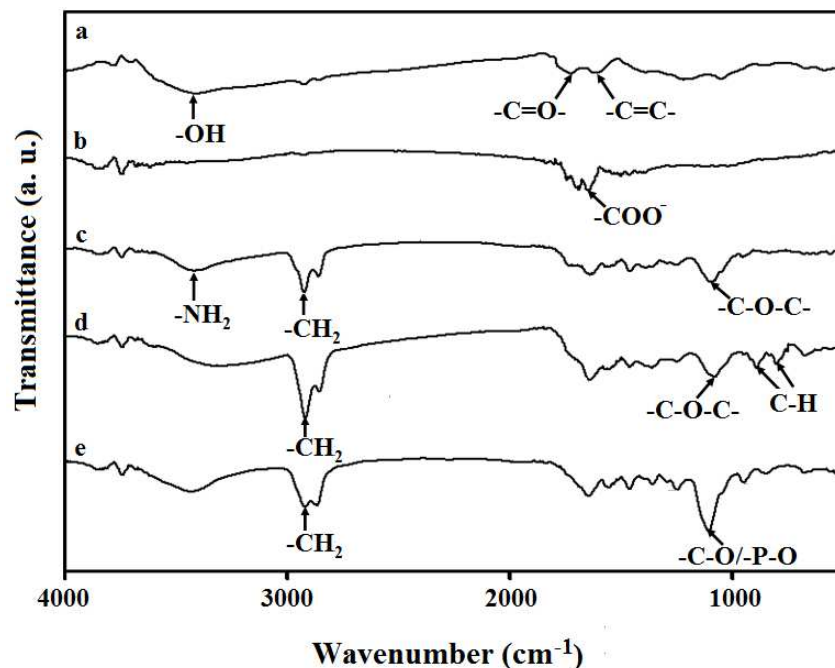


Figure S3. FT-IR spectra of GO derivatives. a) GO, b) carboxylated GO, c) PEGylated GO, d) PEGylated GO with folate modifiers, e) aptamer-PEGylated GO nanoassembly.

The appearance of characteristic absorption peaks at 3400, 1700, and 1580 cm^{-1} (stretching vibrations of O-H, C=O, and C=C, respectively) revealed the presence of -OH, -C=O and -C=C- functional groups in GO. Carboxylated GO showed an increased absorption band at 1630 cm^{-1} and a decreased peak at 3400 cm^{-1} as compared to GO, indicating the conversion of -OH and other functional groups to -COOH on GO. After PEGylation, the GO gave increased characteristic absorption peaks at 3400 cm^{-1} (stretching vibration of N-H), 2925 cm^{-1} (stretching vibration of CH_2) and 1090 cm^{-1} (stretching vibration of C-O-C), suggesting the conjugation of PEG to GO. The PEGylated GO with folate modifiers showed increased absorption peaks at 2923 cm^{-1} (stretching vibration of $-\text{CH}_2-$), 880 cm^{-1} and 795 cm^{-1} (out-of-plane bending of C-H in aromatic rings), confirming the conjugation of folate on PEGylated GO. Aptamer-PEGylated GO nanoassembly gave an increased sugar-phosphate band at 1090 cm^{-1} (P-O or C-O stretching vibration of the ribose-phosphate bond), indicating the successful formation of the nanoassembly.

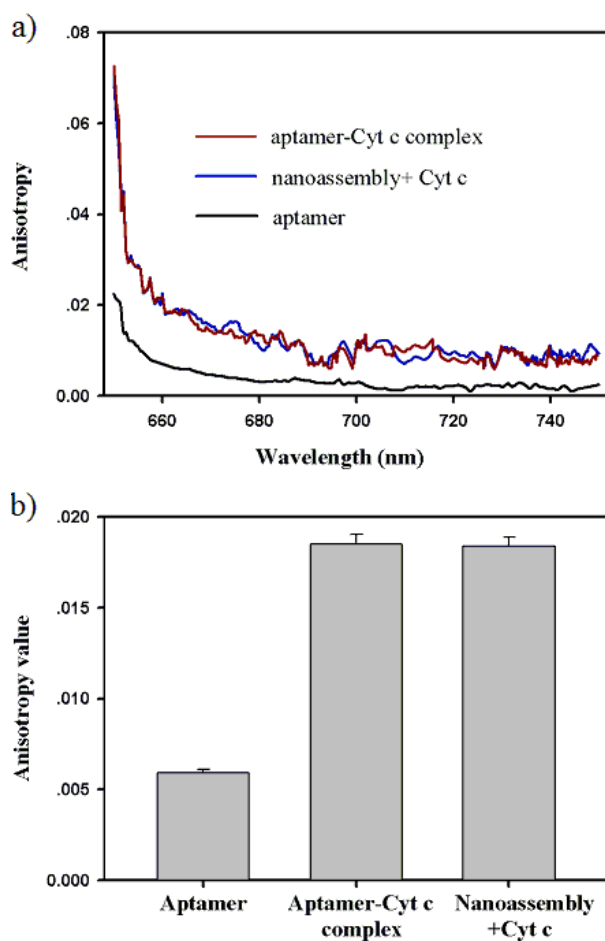


Figure S4. a) Fluorescence anisotropy spectra obtained in interaction assay for Cyt c with the aptamer–PEGylated GO nanoassembly and the DNA aptamer. b) Fluorescence anisotropy values at the maximum emission wavelength (664 nm) obtained in the assay.

The aptamer gave a small fluorescence anisotropy value, suggesting its small size and fast rotation rate in solution. The aptamer–Cyt c complex showed a larger fluorescence anisotropy value, which was almost consistent with the mixture of Cyt c and the nanoassembly, implying the interaction of Cyt c with the nanoassembly resulted in the formation the aptamer–Cyt complex rather than the free aptamer in the solution.

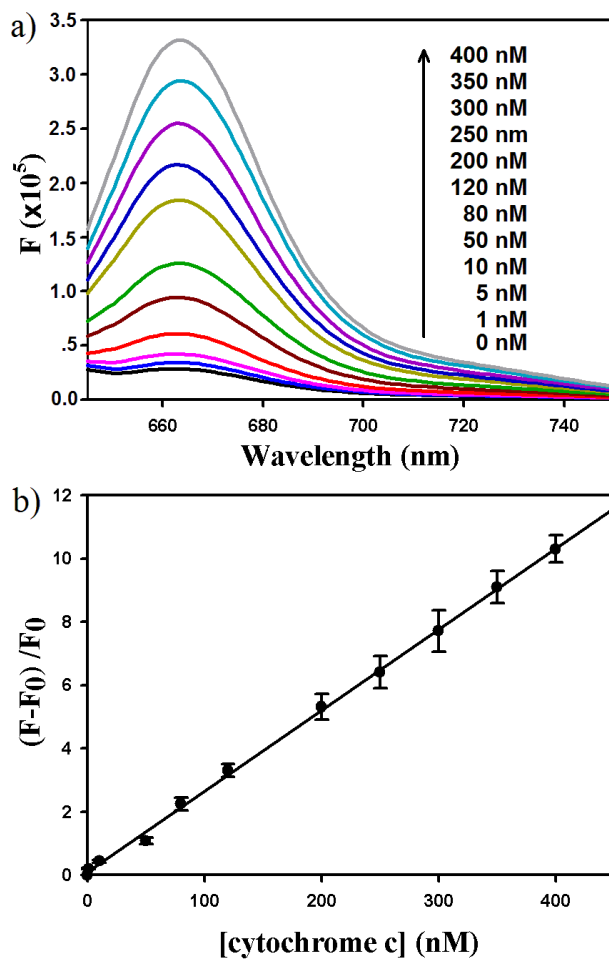


Figure S5. a) Fluorescence spectral responses of the nanoassembly (20 nM aptamer assembled on 6 $\mu\text{g mL}^{-1}$ PEGylated GO) to Cyt c of varying concentrations. b) Correlation curve of normalized fluorescence peak intensities at 664 nm versus Cyt c concentrations. The linear range was from 1 nM to 400 nM with a detection limit of 0.5 nM.

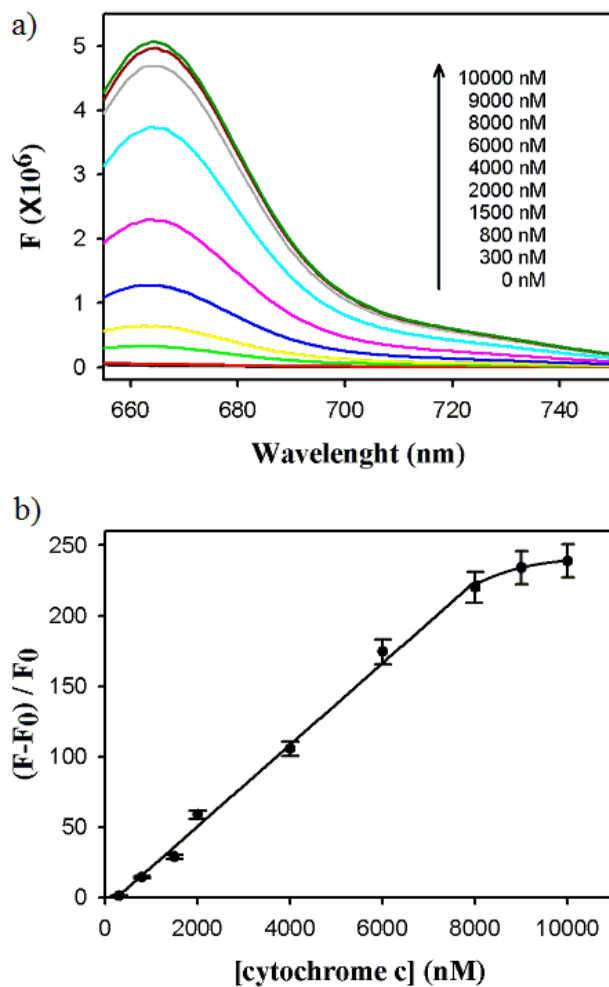


Figure S6. a) Fluorescence spectral responses of aptamer–GO nanoassembly (500 nM aptamer assembled on $50 \mu\text{g mL}^{-1}$ GO) to Cyt c of varying concentrations. b) Correlation curve of normalized fluorescence peak intensities at 664 nm versus Cyt c concentrations. The detection linear ranged from 300 nM to 8000 nM with a detection limit of 100 nM.

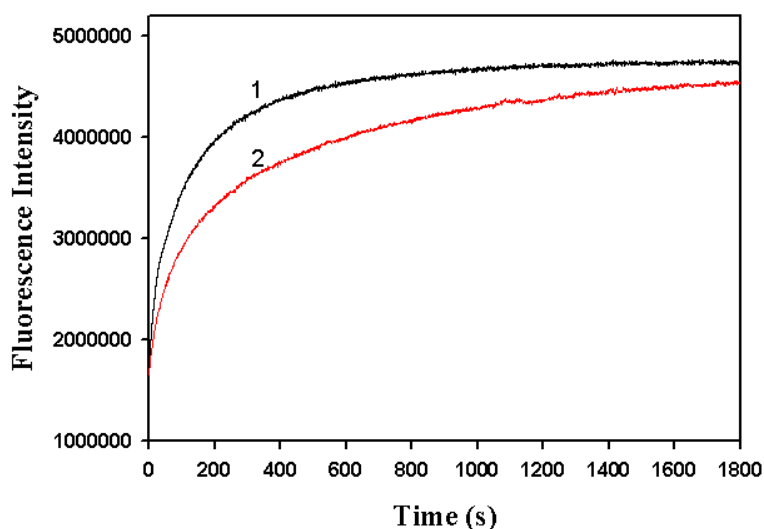


Figure S7. Time-dependent fluorescence peak responses at 664 nm to 10 μM Cyt c using aptamer–PEGylated GO nanoassembly (500 nM aptamer assembled on 150 $\mu\text{g mL}^{-1}$ PEGylated GO, black line) and aptamer–GO nanoassembly (500 nM aptamer assembled on 50 $\mu\text{g mL}^{-1}$ GO, red line).

The result revealed a fast kinetics of the nanosensor in response to Cyt c (90% of the maximum signal was achieved in 280 s and 692 s, respectively, for the aptamer–PEGylated GO nanoassembly and aptamer–GO nanoassembly). The data were further fitted to a first-order kinetic model, which gave estimates of the kinetic rate constants for these nanosensors. The kinetic rate constant was 0.0049 s^{-1} and 0.0022 s^{-1} , respectively, for the aptamer–PEGylated GO nanoassembly and aptamer–GO nanoassembly, suggesting the improvement of the response kinetics by using the nanoassembly with PEGylated GO.

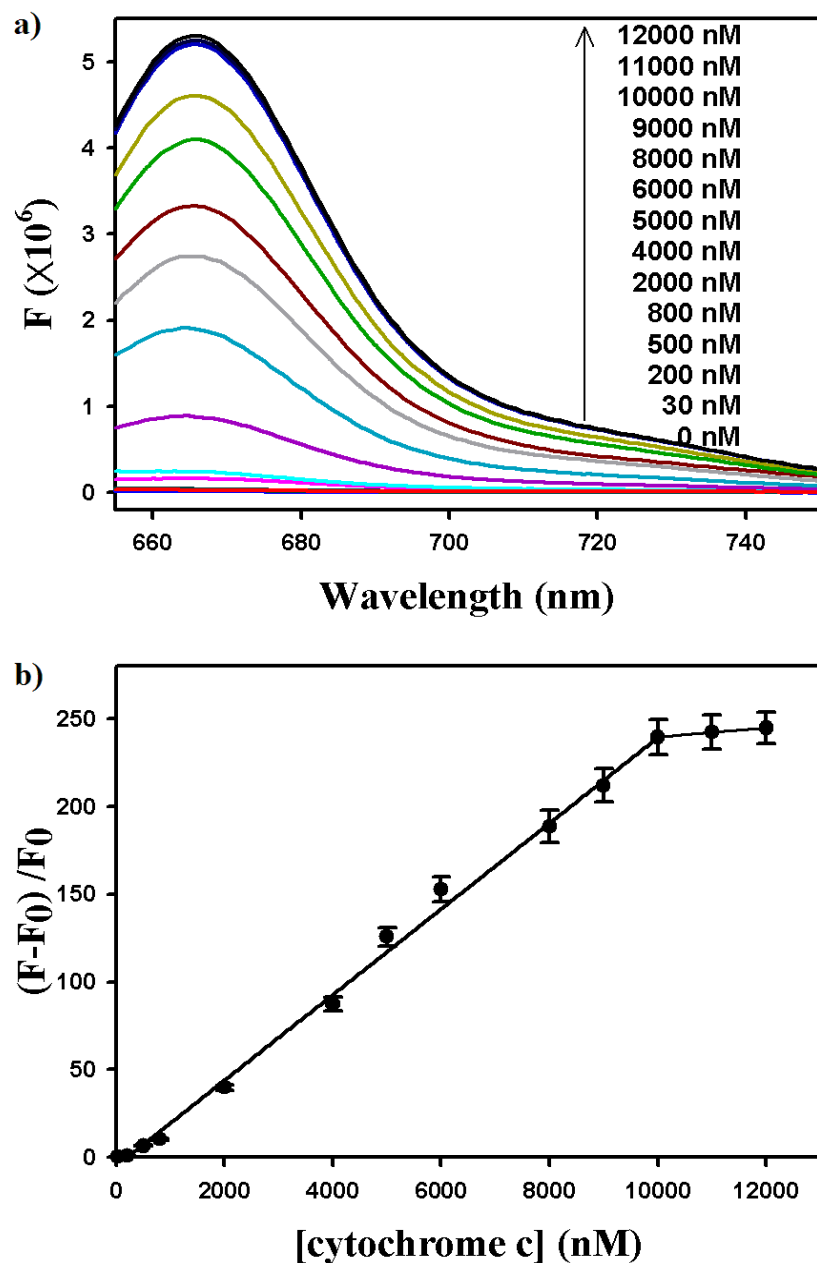


Figure S8. a) Fluorescence spectral responses of the nanoassembly (500 nM aptamer assembled on 150 $\mu\text{g mL}^{-1}$ PEGylated GO) to Cyt c of varying concentrations in the matrix of the plasma extract of non-apoptotic Hela cells. b) Correlation curve of normalized fluorescence peak intensities versus Cyt c concentrations. The linear range was from 30 nM to 10 μM with a detection limit of 10 nM.

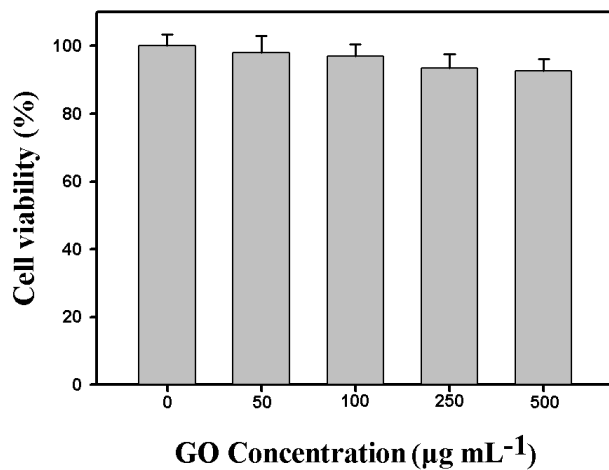


Figure S9. MTT assay of cytotoxicity for aptamer-PEGylated GO nanoassembly. The cell viability values (%) are monitored in HeLa cell lines for varying nanoassembly concentrations (0, 50, 100, 250, 500 µg mL⁻¹ GO) after 8 h incubation.

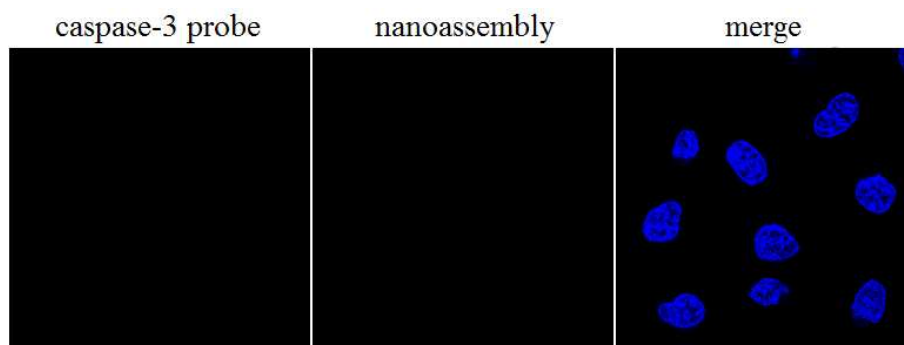


Figure S10. Fluorescence imaging of HeLa cells (FR+) incubated with aptamer-PEGylated GO nanoassembly ($500 \mu\text{g mL}^{-1}$ GO) and $9 \mu\text{M}$ caspase-3 probe in serum-free RPMI-1640 medium for 1 h at 37°C .

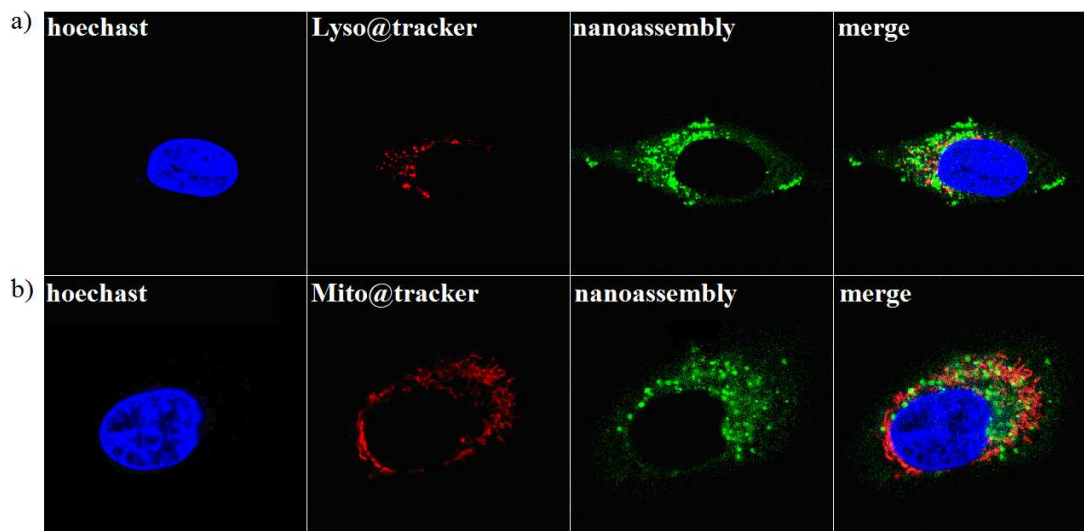


Figure S11. Confocal fluorescence images for localization analysis of aptamer-PEGylated GO nanoassembly with FAM and folate modifiers in HeLa cells (FR+). a) Cells incubated with $15 \mu\text{g mL}^{-1}$ nanoassembly for 1 h and 20 nM lysosome tracker (Lyso@tracker), b) Cells incubated with $15 \mu\text{g mL}^{-1}$ nanoassembly for 1 h and 20 nM mitochondria tracker (Mito@tracker).

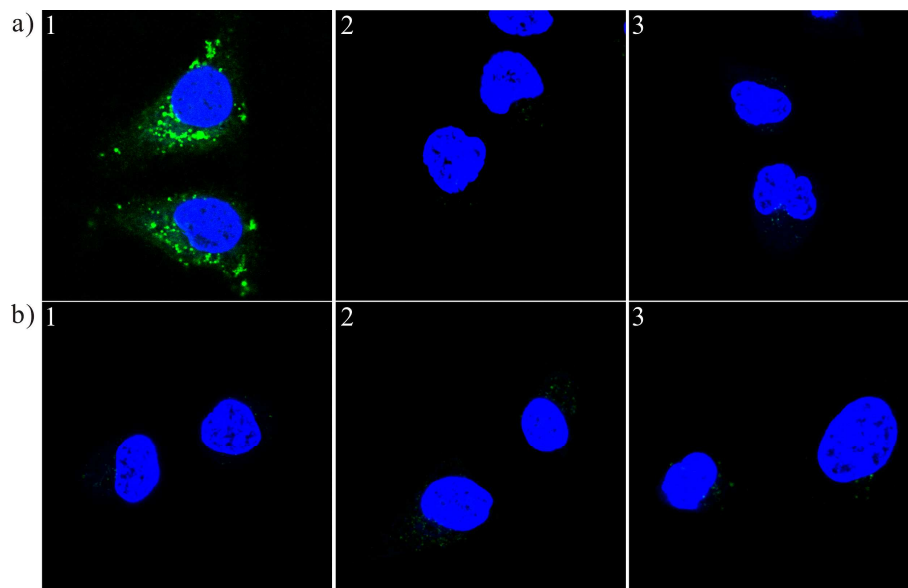


Figure S12. Confocal fluorescence images for intracellular internalization of $15 \mu\text{g mL}^{-1}$ aptamer-PEGylated GO nanoassembly with FAM and folate modifiers (a) and only with FAM modifiers (b). 1) HeLa cells (FR+), 2) HeLa cells (FR-), 3) MCF-7 cells (normally FR-).

The result revealed that the nanoassembly with FAM and folate modifiers was selectively and efficiently uptaken in FR+ cells, and the nanoassembly without folate modifiers showed low efficiency in internalization into cells (FR+ or FR-).

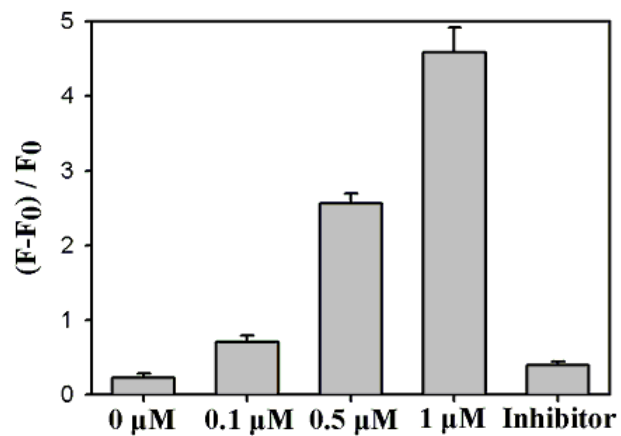


Figure S13. Fluorescence responses of the nanosensor in cytosol extracts (using centrifugal filter devices at 4 °C for 10 times before the experiment) from cells treated with different concentrations of STS for 1.5 h and cells pretreated with 100 μM pepstatin A (Inhibitor) followed by 1 μM STS for 1.5 h.

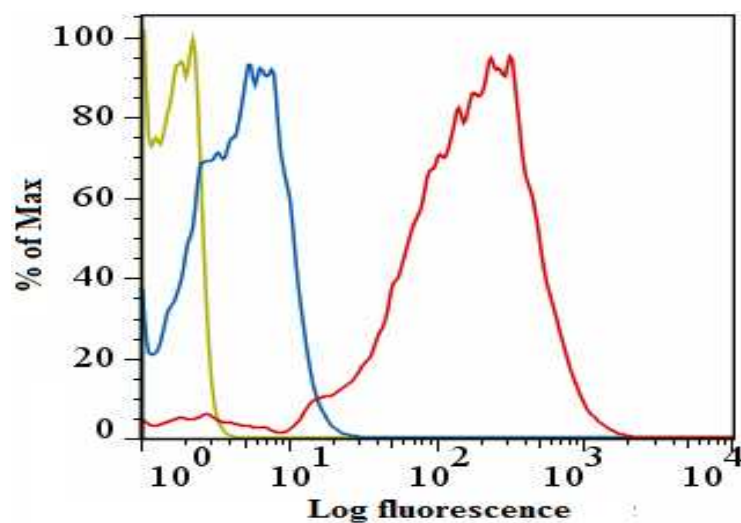


Figure S14. Flow cytometric assay for HeLa cells (FR+): HeLa cells (yellow), HeLa cells incubated with $15 \mu\text{g mL}^{-1}$ nanoassembly for 1 h (blue), cells incubated with $15 \mu\text{g mL}^{-1}$ nanoassembly for 1 h followed by $1 \mu\text{M}$ STS induction for 0.5 h (red).

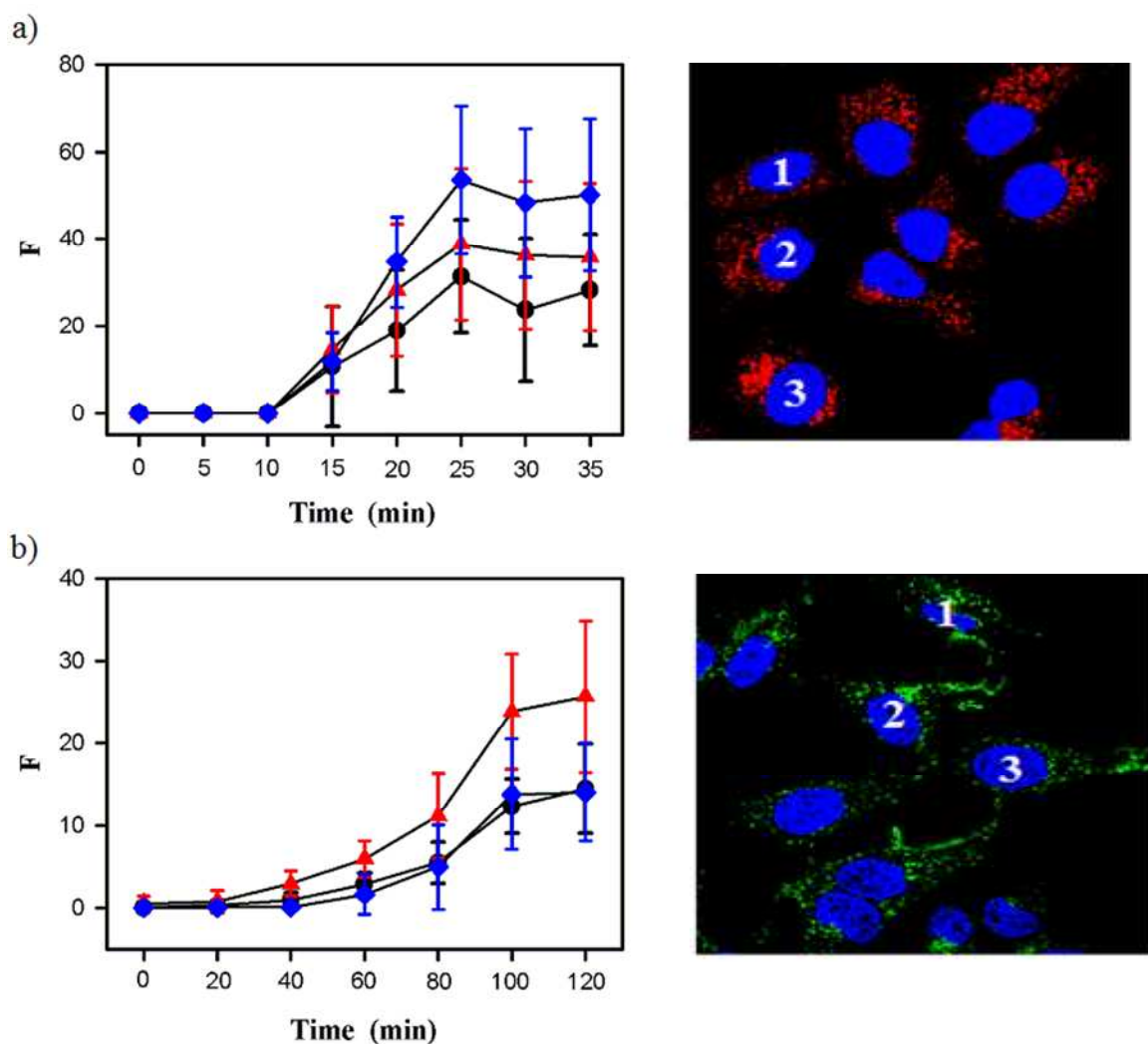


Figure S15. Time-dependent fluorescence intensities obtained from the observed HeLa cells (FR+). a) cells incubated with $15 \mu\text{g mL}^{-1}$ nanoassembly for 1 h followed by imaging on treatment using $1 \mu\text{M}$ STS, b) cells incubated with $9 \mu\text{M}$ caspase-3 probe for 1 h followed by imaging on treatment using $1 \mu\text{M}$ STS. The images, the same as the last ones in Figure 5, are shown for indicating the selected cells marked by the numbers. Each data point is the average from five regions of interest (ROIs) inside the single cell marked in the images (1, black dot, 2: red triangle, 3: blue diamond). The error bars are the standard deviations.

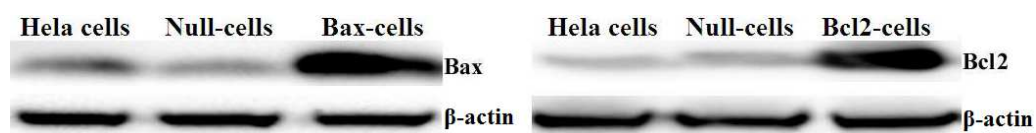


Figure S16. Western blotting assay of the B cell lymphoma 2 (BCL-2) protein family, Bax and Bcl-2, in the extracts from HeLa cells transduced with the recombinant adenovirus containing Bax or Bcl-2 as well as the null control adenovirus containing no exogenous genes. A housekeeping protein β -actin was chosen as the reference.

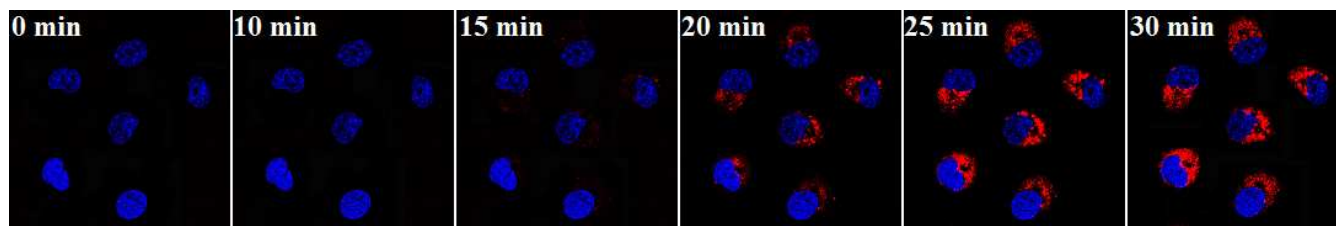


Figure S17. Merge of real-time fluorescence images of cell apoptosis in HeLa cells (FR+) transduced with the null control adenovirus. The cells were incubating with $15 \mu\text{g mL}^{-1}$ nanoassembly for 1 h followed by treatment of $1 \mu\text{M}$ STS for 30 min, and images were obtained at red channel for the nanoassembly and the blue channel for hoechst 33342 nuclear staining.

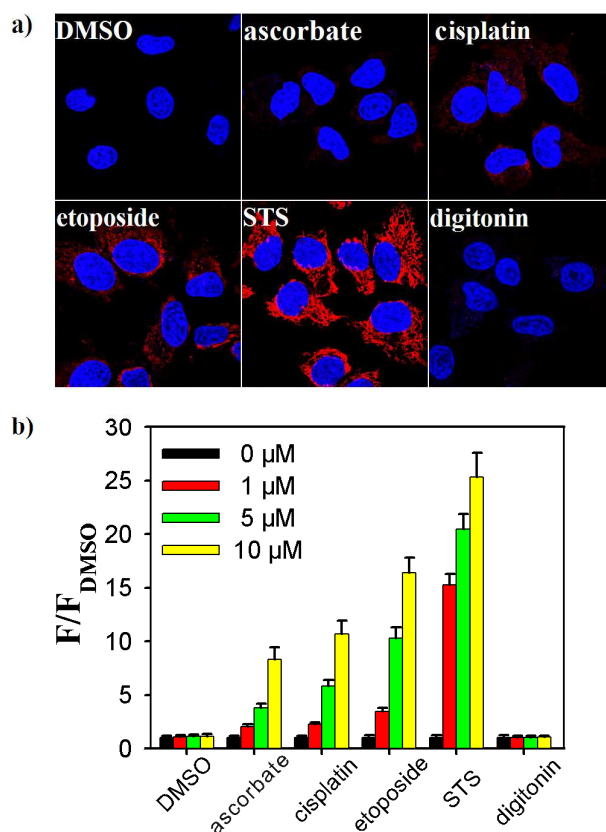


Figure S18. a) Fluorescence imaging of HeLa cells (FR+). The cells were incubated with $15 \mu\text{g mL}^{-1}$ nanoassembly for 1 h followed by treatment of $5 \mu\text{M}$ individual candidate compound (DMSO, sodium ascorbate, cisplatin, etoposide, STS and digitonin) for 1.5 h, and images were obtained at red channel for the nanoassembly and blue channel for hoechst 33342 nuclear staining. b) Relative fluorescence intensities (ratios of average fluorescence response for target compound to that for DMSO at red channel) obtained with different compound concentrations. Each data point is the average from eight regions of interest (ROIs) inside the cells. The error bars are the standard deviations.

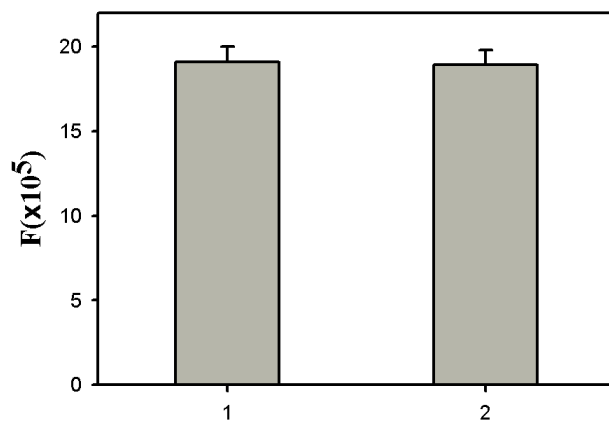


Figure S19. Fluorescence Intensity of (1) 50 nM aptamer, (2) nanoassembly (50 nM aptamer assembled on 15 $\mu\text{g mL}^{-1}$ PEGylated GO) mixed with cytoplasmic extract buffer for 10 min.